Hindawi Publishing Corporation
Journal of Thermodynamics
Volume 2015, Article ID 268034, 11 pages
http://dx.doi.org/10.1155/2015/268034

Research Article

Thermal-Hydraulics Study of a 75 kWth Aqueous Homogeneous Reactor for ^{99}Mo Production

Daniel Milian Pérez,[1] Daniel E. Milian Lorenzo,[1] Lorena P. Rodriguez Garcia,[1] Manuel Cadavid Rodríguez,[2] Carlos A. Brayner de Oliveira Lira,[3] Carlos R. García Hernández,[1] and Jesús Salomón Llanes[1]

[1]*Higher Institute of Technologies and Applied Sciences (InSTEC), Avenida Salvador Allende y Luaces, Quinta de Los Molinos, Plaza de la Revolución, 10400 Havana, Cuba*
[2]*Tecnología Nuclear Médica SpA (TNM), Latadia, Las Condes, 4250 Santiago, Chile*
[3]*Departamento de Energía Nuclear, Universidad Federal de Pernambuco (UFPE), Cidade Universitária, Avenida Professor Luiz Freire, 1000 Recife, PE, Brazil*

Correspondence should be addressed to Daniel Milian Pérez; dperez@instec.cu

Received 12 September 2015; Revised 24 November 2015; Accepted 2 December 2015

Academic Editor: Pedro Jorge Martins Coelho

^{99m}Tc is a very useful radioisotope, which is used in nearly 80% of all nuclear medicine procedures. ^{99m}Tc is produced from ^{99}Mo decay. A potentially advantageous alternative to meeting current and future demand for ^{99}Mo is the use of Aqueous Homogeneous Reactors (AHR). In this paper, a thermal-hydraulics study of the core of a 75 kWth AHR conceptual design based on the ARGUS reactor for ^{99}Mo production is presented. As the ARGUS heat removal systems were designed for working at 20 kWth, the main objective of the thermal-hydraulics study was evaluating the heat removal systems in order to show that sufficient cooling capacity exists to prevent fuel solution overheating. The numerical simulations of an AHR model were carried out using the Computational Fluid Dynamic (CFD) code ANSYS CFX 14. Evaluation shows that the ARGUS heat removal systems working at 75 kWth are not able to provide sufficient cooling capacity to prevent fuel solution overheating. To solve this problem, the number of coiled cooling pipes inside the core was increased from one to five. The results of the CFD simulations with this modification in the design show that acceptable temperature distributions can be obtained.

1. Introduction

^{99m}Tc is a very useful radioisotope, which is used in about 30–40 million procedures worldwide every year [1]. These procedures represent approximately 80% of all nuclear medicine procedures [2]. Currently, ^{99m}Tc is almost exclusively produced from the beta-decay of its 66 h parent ^{99}Mo. At present, most of the world's supply of ^{99}Mo for medical isotope production results from the fission reaction of ^{235}U targets with a fission yield of about 6.1% in multipurpose research reactors. After irradiation in the reactor, the target is processed and ^{99}Mo is recovered through a series of extraction and purification steps using a costly complex of hot cells and auxiliary facilities in order to protect the environment from volatile fission by-products such as iodine, xenon, krypton, and tritium [3]. A main disadvantage of this method results from the large amounts of high activity wastes generated during the target processing [4].

^{99}Mo production system in Aqueous Homogeneous Reactors (AHR) offers a potentially advantageous method of ^{99}Mo production because not only can all of the ^{99}Mo be extracted from the fuel solution [5] but also its low cost, small critical mass, inherent passive safety, and simplified fuel handling, processing, and purification characteristics can be extracted [6]. Over 30 solution reactors have been built and operated around the world with a thermal power ranging from 0.05 W to 5 MW. Although most of these reactors are no longer in service, they accumulate 149 years of combined

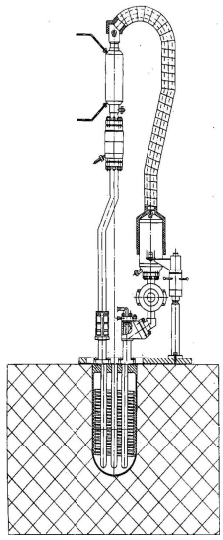

Figure 1: Scheme of the Russian ARGUS reactor [10].

experience [6]. Mainly, three types of aqueous fuel solutions have been considered or used for ^{99}Mo production using an AHR: (1) uranium nitrate [$UO_2(NO_3)_2$], (2) uranium sulphate [UO_2SO_4] [4, 7], and (3) uranium fluoride [UO_2F_2]. In AHR, because of the radiolytic decomposition of the fuel solution, bubbles will be produced. The production of these bubbles will play an important role in the reactor behavior because of the diminution of the density of the fuel solution and the expansion of fuel solution volume [8, 9]. Therefore, the rate and composition of these bubbles must be considered for the design and operation of AHR.

At the present time, the only large scale experiment on the use of an AHR in steady-state operation is the highly enriched uranium (HEU) Russian ARGUS reactor (Figure 1), which operates since 1981 at a maximum power density of 1 kW/L of solution (20 kWth) [6] at the Russian Research Centre "Kurchatov Institute" (RRC KI). After neutron-physical and thermal-hydraulic feasibility calculations for its conversion to low enriched uranium (LEU) fuel during 2010–2012 [10], the ARGUS reactor reached first criticality with LEU fuel in July 2014 [11].

Most studies on AHR have been carried out on the neutron-physical characteristics of these systems and the information available about thermal-hydraulics studies is limited [13–15]. This paper is focused on the thermal-hydraulics study of the core of a 75 kWth AHR [16] (Figure 2) based on the ARGUS reactor LEU configuration [7, 8] using ANSYS CFX 14 code and an AHR model consisting of the vessel, the core channels, the coiled cooling pipe, the fuel solution, and the upper air zone. The increase in the thermal power from 20 kWth to 75 kWth was aimed at to increase the production of ^{99}Mo in order to fulfill a certain demand of ^{99}Mo, considering that the production of ^{99}Mo is proportional to the reactor thermal power. As the ARGUS heat removal systems were designed for working at 20 kWth, the main objective of the thermal-hydraulics study was evaluating the heat removal systems in order to show that sufficient cooling capacity exists to prevent fuel solution overheating. Aspects related with the thermal-hydraulics behavior such as the temperature distributions and the velocity profiles in the fuel solution and other core regions are evaluated. In addition, the dependence of the fuel solution temperature on the radiolytically produced gas bubbles is investigated.

2. Materials and Methods

2.1. Computer Code Description. The CFD calculations were carried out with the CFD code ANSYS CFX 14. Calculations were performed on the InSTEC-IRL cluster (operating system: Microsoft Windows 64 bits, 48 Intel Computer Nodes, node configuration: 1 × Intel(R) Core(TM) i7-4790 (3.6 GHz, 8 cores), 2 × Intel(R) Core(TM) i7-4770 (3.4 GHz, 8 cores), 6 × Intel(R) Core(TM) i3-4150 (3.5 GHz, 4 cores), 48 GB Memory). ANSYS CFX is a general-purpose CFD software suite that combines an advanced solver with powerful preprocessing and postprocessing capabilities. CFD is a computer-based tool for simulating the behavior of systems involving fluid flow, heat transfer, and other related physical processes. It works by solving the equations of fluid flow (in a special form) over a region of interest, with specified initial and boundary conditions of that region [17]. Methods of CFD assume computation of liquid and gas flows by numerical solution of Navier-Stokes and continuity equations (for turbulent flows, Reynolds equations) which describe the most general case of movement of fluid medium. In the present work, momentum, mass, and energy conservation equations as well as the k-ε (turbulent kinetics energy "k" and the turbulent dissipation "ε") model have been used.

2.2. AHR Description

2.2.1. One Coiled Cooling Pipe Conceptual Design. The proposed reactor core conceptual design [16] (based on the ARGUS reactor LEU configuration [10, 11]) (Figure 3) consists of an aqueous uranyl sulphate solution located in a steel cylindrical vessel with a hemispherical bottom. Placed inside the vessel, there are a coiled-tube heat exchanger and one central channel and 2 symmetric peripheral channels (Figure 4). The main reactor core parameters are shown in Table 1. This reactor has an inherent safety determined by the negative power reactivity effect, by the opportunity of cooling down due to the natural air convection, and by the lack of local overheating, low temperature of the solution (up to 363.15 K), and pressure in the reactor vessel (below the atmospheric pressure) [10].

The uranium concentration is 390 g/L and the core volume is 25.5 liters, giving a fuel solution height of 44.02 cm. The amount of ^{235}U in the whole reactor is 1.96 kg. The planned power density is 2.94 kWth/L of solution and the operating temperature of the uranium solution is less than 90°C. The internal coiled-tube heat exchanger is used at about 19 meters of stainless steel tubing, 0.6 cm of inner diameter, and 1.0 cm of outer diameter with inlet water at 20°C. The area of the tubing is about 5970 cm^2. The distilled water flow rate was set up equal to 0.2 kg/s.

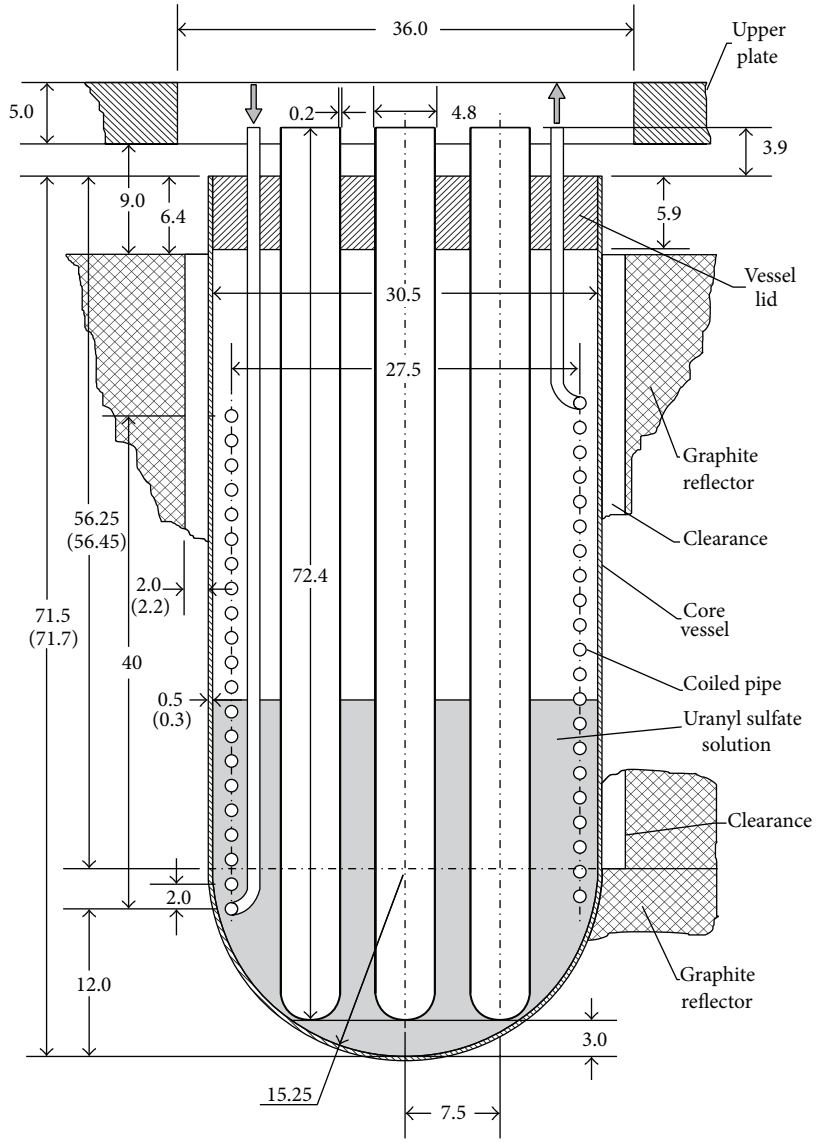

Figure 2: Schematic drawing of the longitudinal section of the assembly core [12].

Table 1: The reactor core parameters.

Parameter	Value
Fuel solution	Uranyl sulphate solution
Uranium concentration (g/L)	~390
Inner core diameter (cm)	30.5
Reactor height (cm)	65.6
Reactor vessel	Stainless steel
Vessel thickness (cm)	0.5
Reflector (radial)	Graphite
Solution density (g/cm^3)	1.4382
Thermal power (kW)	75
Core volume (L)	25.5
Power density (kW/L of solution)	2.94

Figure 5 shows the domains in which the reactor has been divided. Domain 1 is located in the lower part of the reactor and contains the fuel solution. Domain 2 (located above Domain 1) contains the upper air zone. Domain 3 contains the stainless steel coiled cooling pipe.

2.2.2. Five Coiled Cooling Pipes' Conceptual Design. In this configuration, the number of coiled cooling pipes was increased from one to five. Figure 6 shows the location of the new coiled cooling pipes: four near the vessel wall and one around the core central channel. The solution height was increased to 50.385 cm to take into consideration the solution displacement due to the volume of the new pipes. For the five coiled cooling pipes' conceptual design, the area of the tubing is about 21900 cm^2.

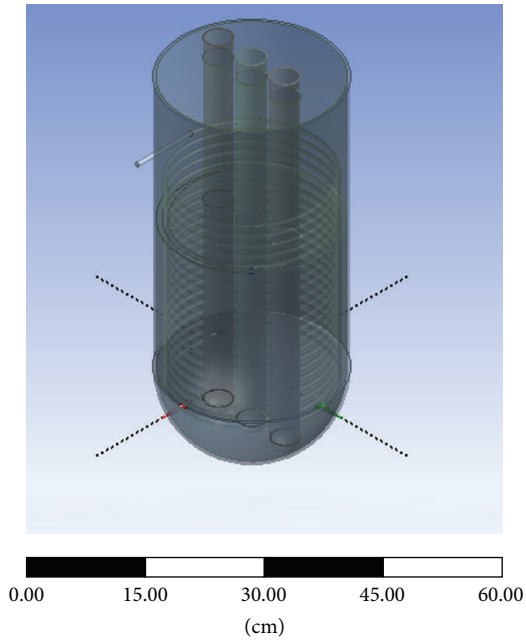

Figure 3: AHR core geometry used in the CFD thermal-hydraulics study.

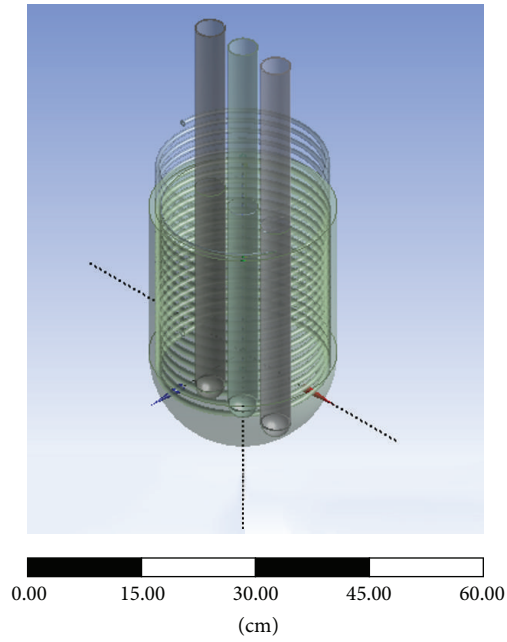

Figure 4: AHR inner structural elements used in the CFD thermal-hydraulics study.

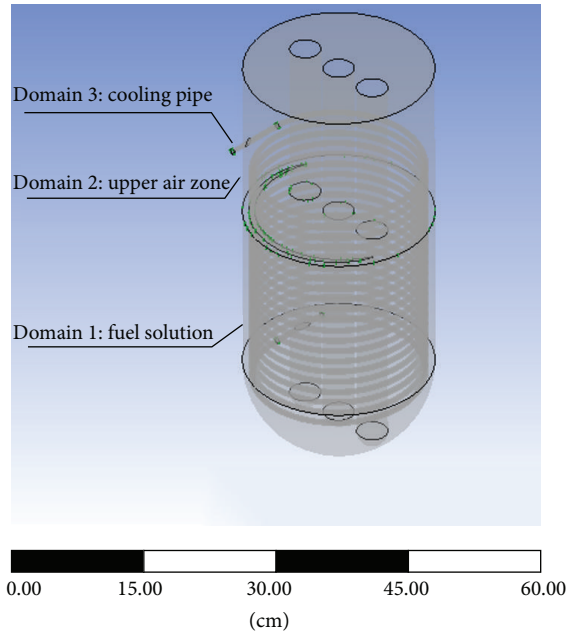

Figure 5: AHR regions used in the CFD thermal-hydraulics study.

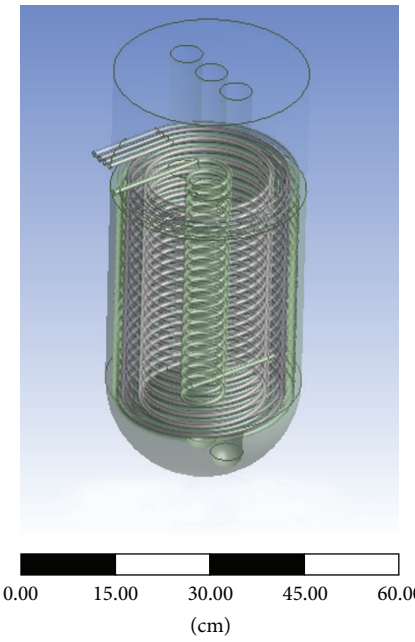

Figure 6: New configuration of the AHR used in the CFD thermal-hydraulics study.

2.3. CFD Model Mesh and Sensitivity Analysis. A preliminary mesh convergence study was carried out in order to verify that the solution is mesh-independent. The number of elements was systematically increased throughout a 1° sector of the core such that six meshes were generated, referred to as "1," "2," "3," "4," "5," and "6" comprising 71746, 94358, 119802, 151403, 183720, and 218868 hexahedral elements, respectively. In the simulations, the two-equation k-ε (Scalable) turbulence model and the high-resolution discretization scheme for the six simulations were used. Figure 7 shows the averaged velocity and temperature distributions in the 1° sector of the core for the six meshes studied. It can be seen that the "5" and "6" meshes give very similar values of averaged velocity and temperature, which differ numerically by less than 1%. Since the differences between the results for the "5" and "6" mesh simulations are minor, the "5" mesh was employed for the simulations performed in this work to

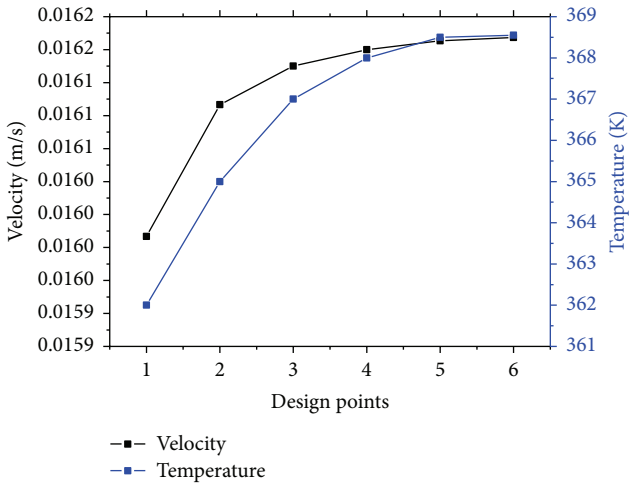

Figure 7: Averaged velocity and temperature distributions for the six different meshes.

Table 2: Mesh details for each domain of the one coiled cooling pipe conceptual design.

Domain	Nodes	Elements
"Air"	560264	3025463
"Coolant"	990819	4554810
"Fuel solution"	1784633	9671224
"Pipe"	1571381	6909971
All domains	4907097	24161468

reduce computational requirements. Figures 8 and 9 show the volumetric temperature and velocity distributions for the "1" and "6" mesh.

In addition, the mesh quality was checked to ensure that values of critical parameters, such as Skewness and Orthogonal Quality, are within recommended limits. Mesh Skewness and Mesh Orthogonal Quality values were around 0.25 and 0.85, respectively, which are an "Excellent" result according to the Skewness mesh metrics spectrum and a "Very Good" result according to the Orthogonal Quality mesh metrics spectrum [17].

The final 360° mesh of the core used in the one coiled cooling pipe conceptual design (Figure 10) contains 4907097 nodes and 24161468 elements. Mesh details for each domain are shown in Table 2. The mesh used in the five coiled cooling pipes' conceptual design contains 4323896 nodes and 23089542 elements.

2.4. Boundary Conditions and Setup. The simulation was calculated as steady state in ANSYS CFX 14 code. The temperature of the distilled water at the cooling coil entrance (inlet) was set up equal to 293.15 K. Turbulence intensity at inlet was assumed to be 5%. A no-slip boundary condition was applied to the rigid walls of the core and the core wall temperature was held at 313.15 K. A free-slip boundary condition was applied to the interface between the fuel solution and the upper air zone. The simulations were done using a uniform volumetric heat generation rate of 75 kW. Further studies should evaluate the use of energy liberation profiles obtained through a neutronic-thermal-hydraulics coupling instead of uniform volumetric heat generation source. The material properties of the coolant (distilled water) and the structural elements (stainless steel) were set according to material model in material library of ANSYS CFX 14. The material properties of the fuel solution (uranyl sulphate) were taken from [18].

Unfortunately, there is insufficient data about the radiolytically produced gas bubbles to evaluate and validate the feedback introduced in the fuel solution for this variable. To reach this goal and considering the scope of this paper, the introduction of the radiolytically produced gas was studied using approaches proposed in [19]. According to these approaches, the introduction of the radiolytically produced gas was modeled as a flow of bubbles from the bottom of the structure with a flow rate equivalent to a volume fraction of 1%. A bubble size of 1 μm was selected as has been proposed in [20, 21].

2.5. Physical Models and Solution Parameters. The two-equation k-ε (Scalable) model and the high-resolution discretization scheme were used to study the behavior of the modeled fluids. K-epsilon (k-ε) is a two-equation turbulence model, which gives a general description of turbulence by means of two transport equations. It is a semiempirical model based on model transport equations for the turbulence kinetic energy (k) and its dissipation rate (ε). The first transported variable determines the energy in the turbulence and the second transported variable determines the rate of dissipation of the turbulent kinetic energy [17]. As the kinetic energy effects are very significant inside the cooling coil, the Heat Transfer Model Total Energy was used. This models the transport of enthalpy and includes kinetic energy effects through a fluid domain. Taking into account the gravity importance, the Buoyancy Model was included in the simulation through the inclusion of a buoyancy source term. The convergence criteria for mass, momentum, energy, and turbulence parameters were set to 10^{-4}.

2.6. Heat Transfer Coefficients. To determine the amount of free-convective heat flow from the fuel solution and air to the cylindrical wall, Evans and Stefany correlation for heating or cooling in closed vertical or horizontal cylindrical enclosures was used in which $0.75 < L/D < 2.0$ (1) [22]. Grashof number is formed with the cylinder length and the fluid properties are evaluated at $T_f = (T_s + T_\sim)/2$:

$$\mathrm{Nu}_D = \frac{hD}{k} = 0.55\left(\mathrm{Gr}_L\mathrm{Pr}\right)^{1/4}. \quad (1)$$

For the free convection inside the spherical cavity a correlation given by F. Kreith was used (2) [22]. In this correlation, Grashof number is based on the cavity diameter and the fluid properties are evaluated at the mean film temperature:

$$\mathrm{Nu}_D = \frac{hD}{k} = 0.59\left(\mathrm{Gr}_D\mathrm{Pr}\right)^{1/4}$$

$$\text{For } 10^4 < \mathrm{Gr}_D\mathrm{Pr} < 10^9,$$

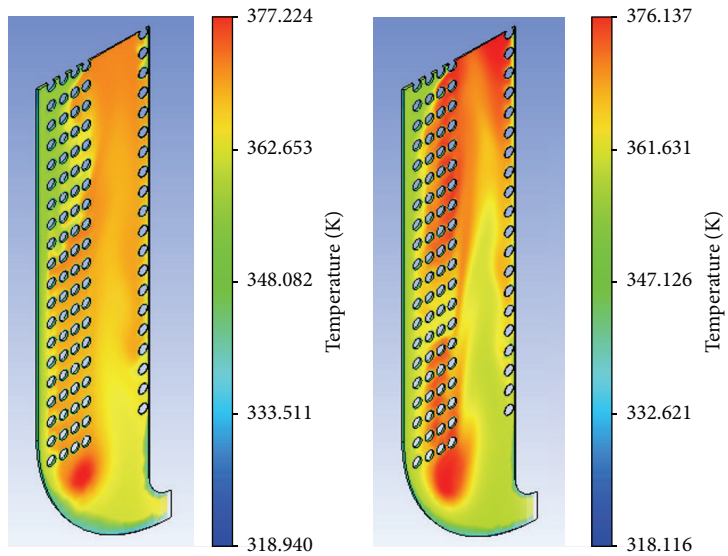

Figure 8: Volumetric temperature distributions for the Design Points 1 and 6.

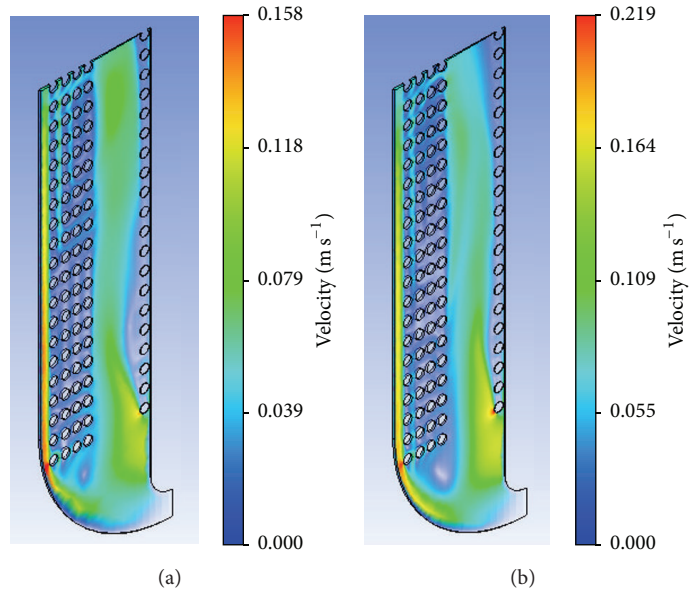

Figure 9: Volumetric velocity distributions for the Design Points 1 and 6.

$$\mathrm{Nu}_D = \frac{hD}{k} = 0.13\left(\mathrm{Gr}_D\mathrm{Pr}\right)^{1/3} \quad \text{For } 10^9 < \mathrm{Gr}_D\mathrm{Pr} < 10^{12}. \tag{2}$$

To determine the amount of free-convective heat flow from the fuel solution and air to the cylindrical channels, Eckert and Jackson correlation for vertical cylinders was used [23]:

$$\mathrm{Nu}_L = \frac{hL}{k} = 0.555\left(\mathrm{Gr}_L\mathrm{Pr}\right)^{1/4} \quad \text{For } \mathrm{Gr}_L\mathrm{Pr} < 10^9,$$
$$\mathrm{Nu}_L = \frac{hL}{k} = 0.021\left(\mathrm{Gr}_L\mathrm{Pr}\right)^{2/5} \quad \text{For } \mathrm{Gr}_L\mathrm{Pr} > 10^9. \tag{3}$$

To determine the amount of free-convective heat flow from the fuel solution and air to the cooling coil, Churchill and Chu correlation was used [24]:

$$\mathrm{Nu}_L = \frac{hL}{k} = \left[0.6 + \frac{0.387\mathrm{Ra}^{1/6}}{\left[1 + (0.559/\mathrm{Pr})^{9/16}\right]^{8/27}}\right]^2 \quad \text{For } \mathrm{Ra} < 10^{12}. \tag{4}$$

To determine the amount of heat flow from the fuel solution and air to the coolant, Dittus-Boelter correlation for a straight tube was used (5) [24]. This correlation was corrected for the coiled tube by multiplying h by $[1 + 3.5(D/D_H)]$, where D is

Table 3: Minimum, maximum, and average temperatures of the fuel solution.

Number	Minimum temperature (K)	Maximum temperature (K)	Average temperature (K)
1	312.80	328.88	321.56
2	314.28	328.50	322.46
3	313.13	328.34	322.83
4	314.72	327.74	322.86

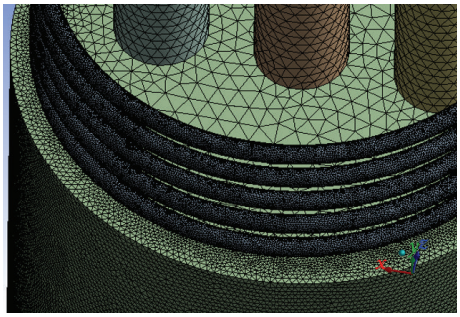

Figure 10: CFD mesh used in the thermal-hydraulics study of the one coiled cooling pipe conceptual design.

the inside diameter of the coil and D_H is the average diameter of the helix:

$$\mathrm{Nu}_L = \frac{hL}{k} = 0.023\mathrm{Re}^{4/5}\mathrm{Pr}^n, \quad (5)$$

where $n = 0.4$ for heating ($T_s > T_m$), $n = 0.3$ for cooling ($T_s < T_m$).

3. Verification of the Models

To the best of the authors' knowledge, no results of analysis of the thermal-hydraulics of the ARGUS reactor are available in the literature for be used in validations tasks. However, in [25], it was reported that the ARGUS reactor temperatures range from 303.15 K to 338.15 K. In order to evaluate the prediction capability of the developed models, calculations were made for four critical AHR configurations proposed in [12] at the ARGUS reactor maximum power density of 1 kWth/L. Table 3 shows the simulation results of the four critical AHR configurations studied regarding to minimum, maximum, and average temperatures of the fuel solution. Figures 11(a)–11(d) show the volumetric temperature distribution in the AHR core for a power density of 1 kWth/L.

As the calculated temperatures distributions are in the reported range for the ARGUS reactor for the four critical configurations, it can be concluded that the developed models are able to acceptably predict the thermal-hydraulics behavior of an AHR.

4. Results and Discussion

As the AHR conceptual design heat removal systems are based on the ARGUS reactor, the first step was evaluating the heat removal systems for the ARGUS designed thermal power (20 kWth). Even though this initial study does not constitute a validation task, it contributes to the verification of the developed detailed model of AHR for thermal-hydraulics studies. The volumetric temperature distribution in the AHR core for a uniform volumetric heat generation rate of 20 kWth is presented in Figure 12; the average fuel solution temperature was 348.31 K and the maximum temperature in the core (355.06 K) was located on the top of the fuel solution and is below the design limit of temperature of 363.15 K. The fuel solution temperature should be below 363.15 K to prevent boiling of the solution.

Then the uniform volumetric heat generation rate was increased to 75 kW; for this value, the average temperature in the core reached 393.67 K. This value is above the design limit of temperature of 363.15 K. To solve this problem, the number of coiled cooling pipes inside the core was increased from one to five; for this new configuration, the average fuel solution temperature in the core was 349.19 K. The maximum temperature in the core reached 361.24 K. Figure 13 shows the volumetric temperature distribution in the AHR core and Figures 14 and 15 show the temperature distribution in the central YZ and XY planes. Figure 16 shows the location of the core regions over 353.15 K. The temperature of the hottest spot in the reactor core, located in the lower part of the fuel solution, was about 12.05 K above the average core temperature.

Fuel solution velocity contours and velocity vectors in the central plane of the AHR core are shown in Figures 17, 18, 19, and 20, respectively. The average velocity of the fuel solution reached 0.016 m/s. The maximum velocities values were obtained near the inferior core wall and around the central core channel. The fuel solution velocity, which is directly related with the fuel density variation provoked by the temperature variation, plays a key role in the reactor cooling.

The simulation results show that the heat removal systems provide sufficient cooling capacity to prevent fuel solution overheating. However, the productions of the gas bubbles were not taken into consideration in the simulations. The production of radiolytically produced gas bubbles in this kind of reactor could provoke an increase in the fuel solution temperature. Results presented in [19] suggest that the negative impact of the thermal conductivity of the gas phase had a significant influence on the overall temperature profiles in the AHR core. To obtain the dependence of the fuel solution temperature from the radiolytically produced gas bubbles, the CFD simulation was done using approaches discussed in Section 2.4.

Figure 21 shows the gas bubbles hold-up or permanency in the fuel solution; the average value determined for this

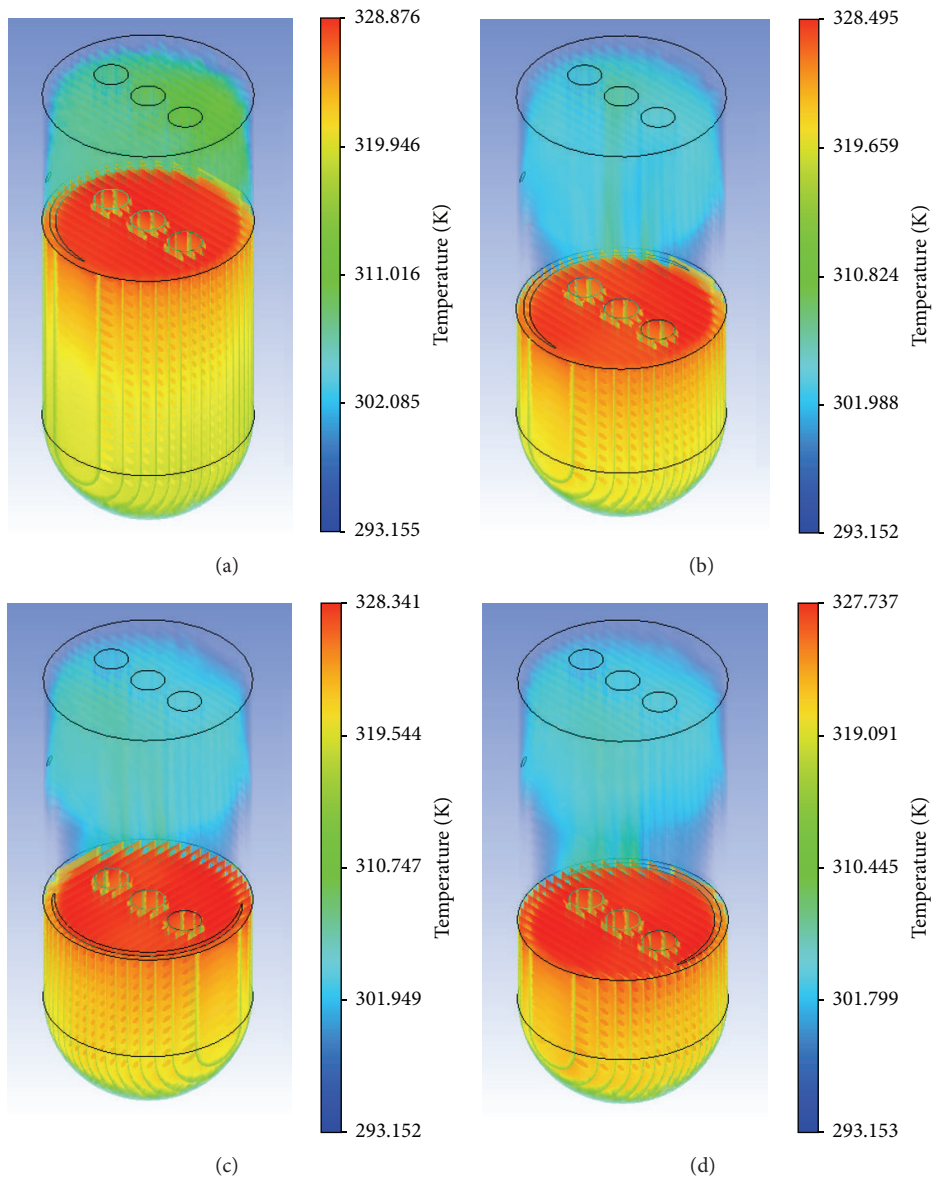

Figure 11: Volumetric temperature distribution in the AHR core.

parameter in the CFD simulation was 7.6%. The average temperature of the fuel solution increases from 349.19 K in the model without gas bubbles to 351.23 K in the model with gas bubbles, while the maximum temperature in the core decreases from 361.24 K in the model without gas bubbles to 355.47 K in the model with gas bubbles. The results obtained show that the presence of gas bubbles causes an increase in the average temperature the fuel solution of about 2 K. However, the presence of gas bubbles allows decreasing the maximum temperature of the fuel solution in 5.75 K from promoting an increase in the fuel solution velocity. The fuel solution velocity increased from 0.016 m/s in the model without gas bubbles to 0.104 m/s in the model with gas bubbles. As the determined temperatures values are below the design limit of temperature of 363.15 K, it can be concluded that the heat removal systems designed for this reactor provide sufficient cooling capacity to prevent fuel solution overheating.

5. Conclusions

The primary objective of this paper is contributing to the thermal-hydraulic analysis of one of the most promissory alternatives to produce medical isotopes: the use of Aqueous Homogeneous Reactors. An AHR conceptual design based on the ARGUS reactor for ^{99}Mo production consisting of the vessel, the core channels, the coiled cooling pipes, the fuel solution, and the upper air zone was developed using ANSYS CFX 14 code.

The main objective of the thermal-hydraulics study was evaluating the heat removal systems in order to show that

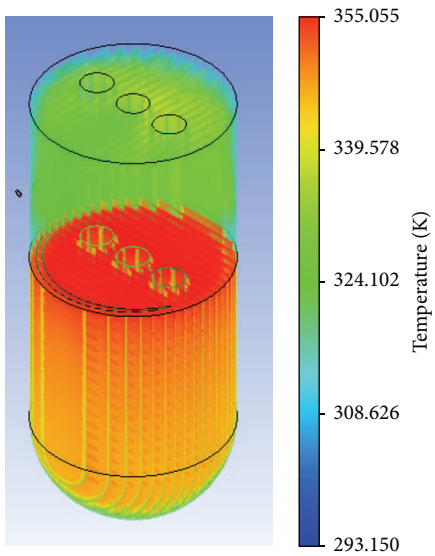

Figure 12: Temperature volume profile in the AHR core with a uniform volumetric heat generation rate of 20 kW.

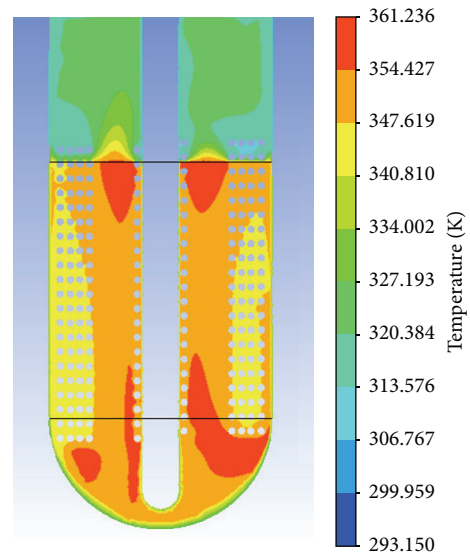

Figure 14: Temperature profile in the central YZ plane of the AHR core.

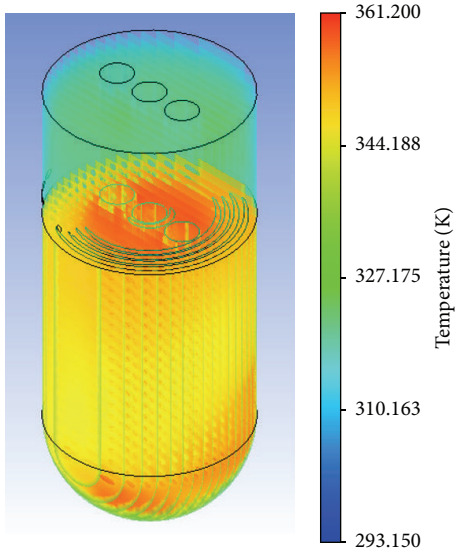

Figure 13: Temperature volume profile in the AHR core with a uniform volumetric heat generation rate of 75 kW.

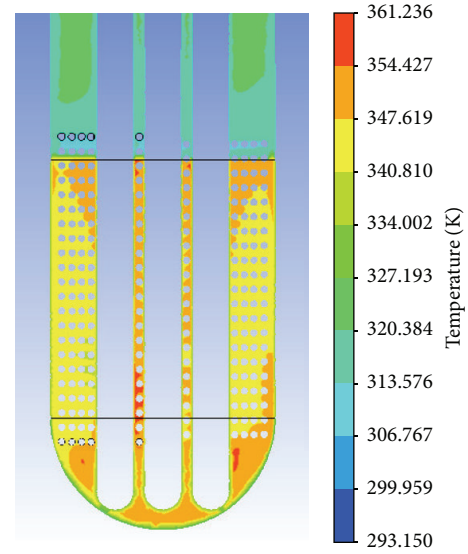

Figure 15: Temperature profile in the central XY plane of the AHR core.

sufficient cooling capacity exists to prevent fuel solution overheating. The calculation results show that the ARGUS heat removal systems, designed for working at 20 kWth, are noy able to provide sufficient cooling capacity to prevent fuel solution overheating after increasing the thermal power to 75 kWth. To solve this problem, the conceptual design was improved, increasing the number of coiled cooling pipes inside the core from one to five. After this modification in the conceptual design, the new heat removal systems provide sufficient cooling capacity to prevent fuel solution overheating; the maximum temperatures reached by the fuel solution (361.24 K in the model without gas bubbles and 355.49 K in the model with gas bubbles) were smaller than the allowable temperature limit (363.15 K). The temperature of the hottest spot in the reactor core was about 4.26 K above the average core temperature in the model with gas bubbles. The presence of gas bubbles in the fuel solution increases the average fuel solution velocity from 0.016 m/s in the model without gas bubbles to 0.104 m/s in the model with gas bubbles.

This study contributes to demonstrating the feasibility of using AHR. However, further investigation and subsequent upgrade of the model used are therefore necessary to confirm these results and contribute to development and demonstration of their technical, safety, and economic viability. Also further studies should evaluate the use of energy liberation

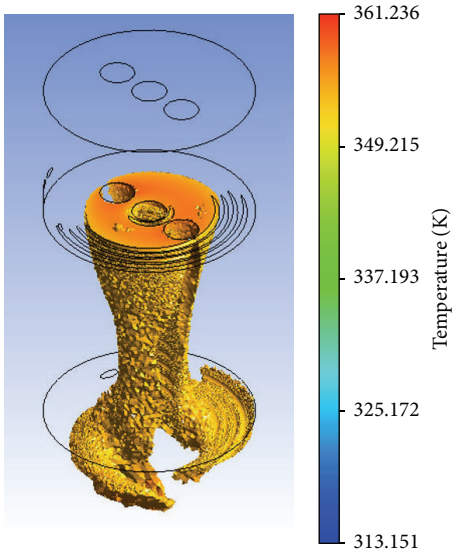

Figure 16: Location of the core regions over 353.15 K.

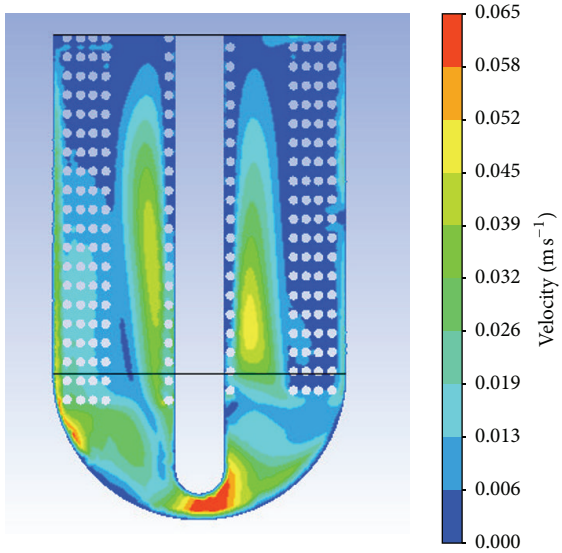

Figure 17: Velocity profile in the central YZ plane of the AHR core.

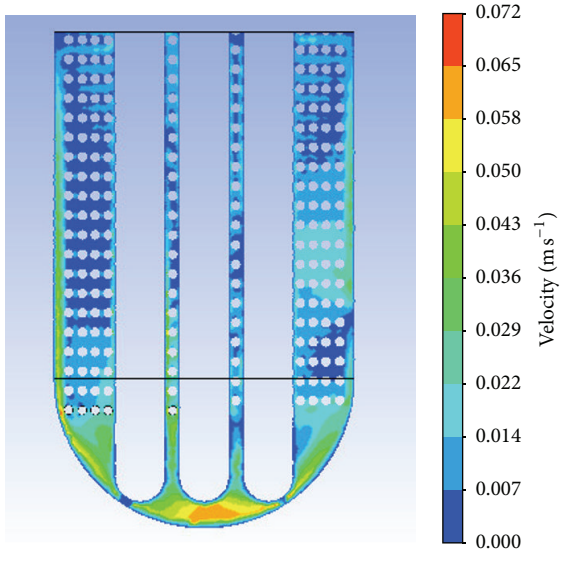

Figure 18: Velocity profile in the central XY plane of the AHR core.

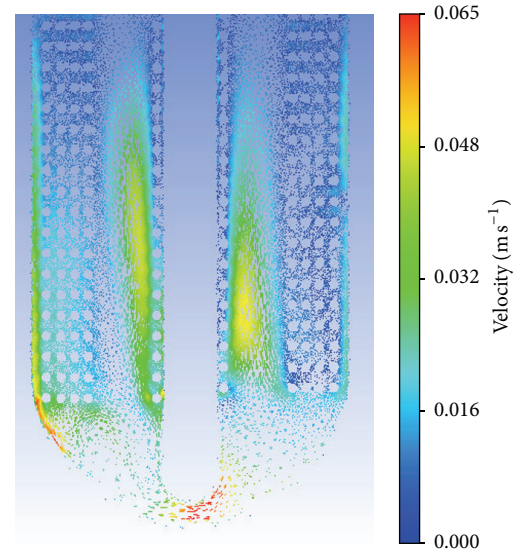

Figure 19: Velocity vectors in the central YZ plane of the AHR core.

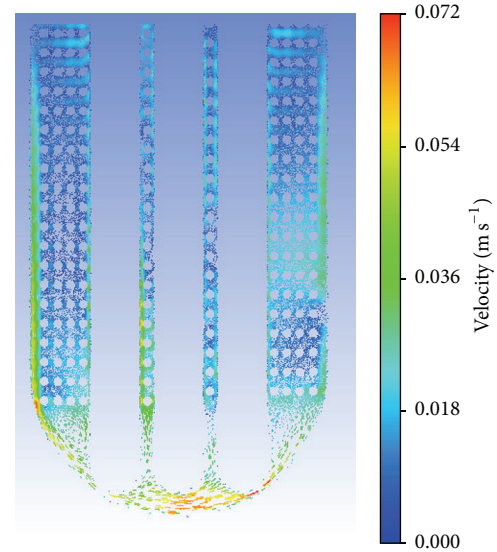

Figure 20: Velocity vectors in the central XY plane of the AHR core.

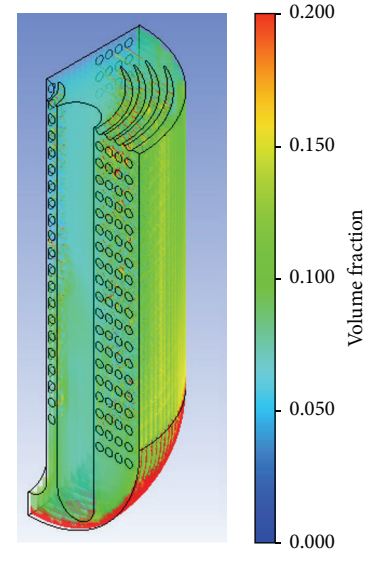

Figure 21: Gas bubbles hold-up in the fuel solution.

profiles obtained through neutronic-thermal-hydraulics coupling instead of uniform volumetric heat generation source.

Nomenclature

Nu: Nusselt number
Gr: Grashof number
Re: Reynolds number
Ra: Rayleigh number
Pr: Prandtl number
k: Thermal conductivity (W/mK)
D: Diameter (m)
L: Length (m).

Conflict of Interests

The authors declare that there is no conflict of interests regarding the publication of this paper.

References

[1] Report to the Nuclear Science Advisory Committee, Review of the NNSA GTRI Mo-99 Program, May 2014.

[2] P. Peykov and R. Cameron, "Medical isotope supply in the future: production capacity and demand forecast for the 99Mo/99mTc market, 2015–2020," Tech. Rep., Nuclear Energy Agency (NEA), 2014.

[3] A. Mushtaq, "Future of low specific activity molybdenum-99/technetium-99m generator," *Current Radiopharmaceuticals*, vol. 5, no. 4, pp. 325–328, 2012.

[4] IAEA, "Non-HEU production technologies for molybdenum-99 and technetium-99m," IAEA Nuclear Energy Series no. NF-T-5.4, IAEA, Vienna, Austria, 2013.

[5] A. Isnaeni, M. S. Aljohani, T. G. Aboalfaraj, and S. I. Bhuiyan, "Analysis of ^{99}Mo production capacity in uranyl nitrate aqueous homogeneous reactor using ORIGEN and MCNP," *Atom Indonesia*, vol. 40, no. 1, 2014.

[6] IAEA, "Homogeneous aqueous solution nuclear reactors for the production of ^{99}Mo and other short lived radio isotopes," Tech. Rep. IAEA-TECDOC-1601, IAEA, 2008.

[7] A. J. Youker, S. D. Chemerisov, M. Kalensky, P. Tkac, D. L. Bowers, and G. F. Vandegrift, "A solution-based approach for Mo-99 production: considerations for nitrate versus sulfate media," *Science and Technology of Nuclear Installations*, vol. 2013, Article ID 402570, 10 pages, 2013.

[8] C. C. Pain, C. R. E. de Oliveira, A. J. H. Goddard, and A. P. Umpleby, "Non-linear space-dependent kinetics for the criticality assessment of fissile solutions," *Progress in Nuclear Energy*, vol. 39, no. 1, pp. 53–114, 2001.

[9] Y. Li, H. Wu, L. Cao et al., "FMSR: a code system for in-core fuel management calculation of aqueous homogeneous solution reactor," *Nuclear Engineering and Design*, vol. 240, no. 4, pp. 763–770, 2010.

[10] S. V. Myasnikov, A. K. Pavlov, N. V. Petrunin, and V. A. Pavshook, "Conversion of the ARGUS solution reactor to LEU fuel: results of feasibility studies and schedule," in *Proceedings of the 34th International Meeting on Reduced Enrichment for Research and Test Reactors (RERTR '12)*, Warsaw, Poland, October 2012.

[11] P. P. Boldyrev, V. S. Golubev, S. V. Myasnikov, A. K. Pavlov, N. V. Petrunin, and V. A. Pavshook, "The Russian ARGUS solution reactor HEU-LEU conversion: LEU fuel preparation, loading and first criticality," in *Proceeding of 35th International Meeting on Reduced Enrichment for Research and Test Reactors (RERTR '14)*, October 2014.

[12] *Graphite-Reflected Uranyl Sulphate (20.9% 235U) Solutions, Volume III*, IEU-SOL-THERM-001, NEA/NSC/DOC/(95)03, 1997.

[13] M. V. Huisman, *Medical Isotope Production Reactor Reactor design for a small sized aqueous homogeneous reactor for producing molybdenum-99 for regional demand [Master Thesis in Applied Physics]*, Delft University of Technology, 2013.

[14] S. Rijnsdorp, *Design of a small aqueous homogeneous reactor for production of 99Mo improving the reliability of the supply chain [M.S. thesis]*, Delft University of Technology, 2014.

[15] C. M. Cooling, *Development of a point kinetics model with thermal hydraulic feedback of an aqueous homogeneous reactor for medical isotope production [Ph.D. thesis]*, Engineering in Nuclear Engineering of Imperial College London and the Diploma of Imperial College London, 2014.

[16] D. Milian, D. E. Milian, M. Cadavid, L. P. Rodriguez, and J. Salomón, "Feasibility neutronic conceptual design for the core configuration of a 75 kWth aqueous homogeneous reactor for 99Mo production," in *Proceeding of XV Workshop on Nuclear Physics and IX Symposium on Nuclear & Related Techniques*, 2015.

[17] ANSYS CFX, release 14, Help System, Meshing User's Guide and CFX Documentation, ANSYS, Inc, 2011.

[18] A. J. Younker, D. C. Stepinski, L. Ling, and F. George, "Mo recovery updates and physical properties of uranyl sulfate solutions," Tech. Rep. ANL/CSE-13/20 REV 1 109440, Report of the Argonne National Laboratory, Chemical Sciences and Engineering Division, 2014.

[19] S. Chemerisov, R. Gromov, V. Makarashvili et al., "Experimental setup for direct electron irradiation of the uranyl sulfate solution: bubble formation and thermal hydraulics studies," in *Proceedings of the Mo-99 Topical Meeting on Molybdenum-99 Technological Development*, Washington, DC, USA, June 2014.

[20] D. Y. Chuvilin, J. D. Meister, S. S. Abalin et al., "An interleaved approach to production of 99Mo and 89Sr medical radioisotopes," *Journal of Radioanalytical and Nuclear Chemistry*, vol. 257, no. 1, pp. 59–63, 2003.

[21] F. J. Souto and R. H. Kimpland, "Reactivity analysis of solution reactors for medical-radioisotope production," *Nuclear Instruments & Methods in Physics Research, Section B*, vol. 213, pp. 369–372, 2004.

[22] D. R. Pitts and L. E. Sissom, *Theory and Problems of Heat Transfer*, McGraw-Hill, New York, NY, USA, 2nd edition, 1997.

[23] E. Cao, *Transferencia de Calor en Ingeniería de Procesos*, 1st edition, 2004.

[24] F. P. Incropera and D. P. DeWitt, *Fundamentals of Heat and Mass Transfer*, John Wiley & Sons, New York, NY, USA, 4th edition, 1996.

[25] D. Yu. Chuvilin, R. W. Brown, V. E. Khvostionov et al., "Experimental demonstration of the new tecnology of medical Sr-89 production in solution reactor," in *Proceedings of the 5th International Conference on Isotopes (ICI '05)*, Brussels, Belgium, April 2005.